Activated carbon from leather shaving wastes and its application in removal of toxic materials

Ismail Cem Kantarli [a], Jale Yanik [b,*]

[a] *Ataturk Medical Technology Vocational Training School, Ege University, 35100 Bornova/Izmir, Turkey*
[b] *Faculty of Science, Department of Chemistry, Ege University, 35100 Bornova/Izmir, Turkey*

ARTICLE INFO

ABSTRACT

In this study, utilization of a solid waste as raw material for activated carbon production was investigated. For this purpose, activated carbons were produced from chromium and vegetable tanned leather shaving wastes by physical and chemical activation methods. A detailed analysis of the surface properties of the activated carbons including acidity, total surface area, extent of microporosity and mesoporosity was presented. The activated carbon produced from vegetable tanned leather shaving waste produced has a higher surface area and micropore volume than the activated carbon produced from chromium tanned leather shaving waste. The potential application of activated carbons obtained from vegetable tanned shavings as adsorbent for removal of water pollutants have been checked for phenol, methylene blue, and Cr(VI). Adsorption capacities of activated carbons were found to be comparable to that of activated carbons derived from biomass.

© 2010 Elsevier B.V. All rights reserved.

1. Introduction

In wastewater treatment, removal of resistant organic compounds and hazardous inorganic material such as the heavy metals is paid a special attention. The effluents from dyes, textile, and pulp and paper industries are densely colored due to the presence of residual dyes which are designed to be resistant to environmental conditions like light, effects of pH and microbial attack and are microtoxic to aquatic life since they significantly affect photosynthetic activity in aquatic life by reducing light penetration [1–3]. Phenol and its derivatives such as methyl phenols, ethyl phenols, and dimethyl phenols constitute a group of pollutants that are invariably present in the effluents from industries engaged in the manufacture of a variety of chemical compounds such as plastics, dyes and plants used for coal gasification, and petrochemical units. Many of these compounds are carcinogenic, even when present in low concentrations. The content of phenolic compounds in the effluents from industries (about 200–2000 mg/l) is usually higher than the standard limits required for their release into aquatic environment [4]. Wastes containing chromium are created in many branches of industry such as tannery, paint, ink, dye, and aluminum manufacturing industries, etc. Chromium in the hexavalent form is a strong oxidant and known to be both acutely and chronically toxic to human [5]. Several physicochemical and biological treatment techniques (solvent extraction, ion exchange by resins,

chemical oxidation by ozone, aerobic or anaerobic biodegradation, etc.) already exist today for removal of these pollutants, but the most effective and frequently used procedure is adsorption on activated carbons.

The tanning industry is familiar with its being a potentially pollution-intensive industry. The environmental impacts from tanneries result from liquid, solid and gaseous waste streams. It must be emphasized that 4 million tones of solid waste per year is generated by the global tannery industry [6]. According to the estimation of Sreeram et al., about 0.8 million tons of chromium tanned shavings are generated per year globally [7]. The solid wastes from tannery industries may have significant Cr(III) content. Even though Cr(III) is viewed as not toxic, possible oxidation of Cr(III) to Cr(VI), due to the acid rains or incineration, threats the environment since Cr(VI) is a more toxic species. Therefore, the conventional disposal methods, land-filling and incineration, cannot be considered a solution to the disposal problem of tanned leather wastes in eco-friendly manner. In literature, there are many studies on the treatment of tanned leather wastes mainly including the extraction of chromium from wastes to re-use in the tanning process [8,9] and isolation of protein fractions [10,11].

In this study, the problems of valorization of leather shaving wastes from tannery industry on one hand, and contamination of aqueous effluents by industrial activities including tannery industry on the other hand, are simultaneously considered. For valorization of leather shaving wastes from tannery industry in an economical and eco-friendly manner, the possibility of using these wastes as an active carbon raw material was investigated. In literature, a few study about production of activated carbon

Table 1
Properties of leather shaving wastes.

Waste type	Proximate analysis, wt%		Ultimate analysis, wt%											
	Moisture	Ash	C	H	N	S	Cl	Cr	Fe	P	Si	Na	K	Ca
CTS	15.4	4.7	37.20	6.40	13.60	1.79	4.11	4.35	0.114	0.025	0.054	0.958	0.047	0.156
VTS	11.9	3.3	46.20	5.50	6.60	1.29	0.575	0.021	0.132	0.031	0.079	0.503	0.981	0.592

from tanned leather wastes by CO_2 activation exist [12–14]. In comparison with those studies, this study covered the chemical and physical activation of leather shaving wastes in detail. For CO_2 activation, the effect of process parameters such as demineralization, activation time, carbonization temperature on surface characteristics of resulting products was investigated. For chemical activation, the effect of carbonization temperature, impregnating agent type and impregnation ratio on surface characteristics of resulting products was examined. In order to consider the problems of contamination of aqueous effluents by industrial activities, potential application of the produced activated carbons in methylene blue, phenol and Cr(VI) removal from aqueous solutions was investigated.

2. Materials and methods

2.1. Solid wastes from tannery industry

Tannery wastes – chromium- and vegetable-tanned leather shavings – (CTS and VTS) used in this study were supplied by Sepiciler Co., Izmir, Turkey. Before carbonization experiments, shaving wastes were shredded into the rectangular pieces (1 cm × 2 cm) and then dried in an oven at 105 °C to constant weight. Proximate and ultimate analyses of these wastes are given in Table 1.

2.2. Production of activated carbon by physical activation

2.2.1. Carbonization

Carbonization of shaving waste was carried out in vertical pyrolysis reactor. Pyrolysis reactor was of a fixed bed design and of stainless steel with 6 cm diameter and 21 cm high. In a typical run, shaving waste of 50–60 g was placed into the reactor. The system was heated to the desired carbonization temperature (450 or 600 °C) at a heating rate of 5 °C/min, and hold at this temperature for 2 h. The volatile products were swept by nitrogen gas (25 ml/min) from reactor. After carbonization, the reactor was cooled under nitrogen gas and the residue in reactor (char) was used in activation processes.

2.2.2. Demineralization and CO_2 activation of chars

The chars were boiled with HCl solution (10 wt%) for 2 h to decrease its inorganic content. After HCl treatment, they were washed with hot water and finally with cold water until no chloride ions could be detected by testing with $AgNO_3$ solution and then dried. Activation of chars was carried out by carbon dioxide. In the activation process, the char, either demineralized or not, was heated to 900 °C under nitrogen atmosphere. As soon as the reactor temperature reached 900 °C, the inert atmosphere was rapidly substituted by flowing carbon dioxide (350 ml/min). At the end of the desired activation time, the reactor was cooled to room temperature under nitrogen atmosphere. The activated carbon from activation process was weighted (m_2) to calculate the burn-off

value. The burn-off value was calculated by

$$\% \, \text{burn-off} = \frac{M - m_2}{M} \times 100$$

where M is the initial mass of char.

2.3. Production of activated carbon by chemical activation

As the first step of chemical activation, 50 g of the dried leather shaving waste was mixed in beaker with 250 ml of H_3PO_4 and $ZnCl_2$ solutions with varying concentrations. H_3PO_4 and $ZnCl_2$ solution was used in impregnation ratios of 0.5:1, 1:1, 1.5:1 and 2:1 of weight of impregnation reagent/weight of waste (referred to as 50, 100, 150 and 200 wt% loading). The slurry was then dried in an oven at 105 °C overnight.

The impregnated waste samples were placed into the vertical pyrolysis reactor and carbonized at 450 or 600 °C as mentioned in Section 2.2.1. After carbonization, the char was boiled with 200 ml of 10% HCl solution for 120 min, filtered in a vacuum flask and washed with hot water and finally cold water to remove the chloride ions and other inorganics.

2.4. Characterization of activated carbons

The equipment used for surface area and pore structure characterization is an accelerated surface area and porosimetry system (Quanthacrome Autosorb 1-C apparatus). Surface area was estimated by applying the Brunauer, Emmett and Teller (BET) equation, while, the micropore volumes were calculated by the t-plot approach [15]. The mesopore volume was calculated according to the BJH theory [16]. The scanning electron micrograph (SEM) analyses were recorded by using PHILIPS XL-30 S FEG SEM instrument. The amount of surface oxygen groups on the activated carbons has been determined by Boehm titration method [17].

2.5. Adsorption experiments

The ability of the activated carbons to remove methylene blue, phenol and Cr(VI) from aqueous solutions was determined under batch-mode conditions. Cr(VI) solutions were prepared by dissolving potassium dichromate in distilled water. The optimum pH values for adsorption experiments were determined with preliminary studies (not presented here). The pH of each Cr(VI) solution was adjusted to optimum value of 2. No pH adjustment was done for methylene blue and phenol solutions. Test solutions (100 ml) of various concentration (ranging between 100–500 mg/l for methylene blue, 50–250 mg/l for phenol and 50–250 mg/l for Cr(VI)) were added to the adsorbent (0.1 g) in flasks and suspensions were shaken for an equilibrium time determined with preliminary studies (24, 4 and 2 h for methylene blue, phenol, and Cr(VI), respectively). The filtrates were analyzed for residual methylene blue and phenol concentration using the UV–visible spectrophotometer (UV-160A, Shimadzu) at 665 nm and 269 nm, respectively. For residual Cr(VI) concentration, the filtrates were analyzed by

Table 2
The effect of activation time on burn-off, BET surface area, pore volumes and average pore sizes of activated carbons from CTS-derived chars.

Carbonization temperature, °C	Char type	Activation time, h	Burn-off, %	BET surface area, m²/g	Micropore volume, cm³/g	Mesopore volume, cm³/g	Total pore volume, cm³/g	Average pore size, Å
450	Non-demineralized	1	41.8	290	0.046	0.244	0.279	38.49
		3	56.1	559	0.105	0.362	0.477	34.13
		4	62.2	795	N.D.	N.D.	N.D.	N.D.
	Demineralized	2	52.2	415	0.106	0.230	0.326	31.45
		3	57.4	796	0.197	0.408	0.609	30.60
		4	62.1	769	0.179	0.384	0.563	29.28
600	Demineralized	2	40.7	457	N.D.	N.D.	N.D.	N.D.
		4	50.2	643	N.D.	N.D.	N.D.	N.D.
		6	60.2	577	N.D.	N.D.	N.D.	N.D.

N.D.: not determined.

reaction with 1,5-diphenylcarbazide followed by absorbance measurement at 540 nm using the UV–visible spectrophotometer.

3. Results and discussion

3.1. Production of activated carbon from chromium tanned leather shaving waste

3.1.1. Physical activation

Before activation, chars obtained from carbonization of CTS were demineralized due to their high ash content. By demineralization, the ash content of 450 and 600 °C chars was decreased from 17.9% and 26.1% to 11.6% and 17.9%, respectively. The HCl washing was not very effective in reducing the ash content of these chars. The reason may be the formation of water- and HCl-insoluble inorganic chromium compounds during carbonization.

Both the non-demineralized and demineralized chars were treated with CO_2 gas at 900 °C for 1–6 h.

The effect of activation time on burn-off, BET surface area and pore volumes of non-demineralized and demineralized chars are given in Table 2. Because of the high burn-off value, the activation times more than 4 h were not tested for the 450 °C chars. Besides, surface properties of activated carbons obtained from 600 °C non-demineralized char were not investigated in detail because of their high ash content.

As seen from Table 2, for the same activation times, burn-off values obtained for 450 °C chars were higher than the burn-off values obtained for 600 °C chars. This may be attributed to the more complete carbonization (less volatile matter content, etc.) at higher temperatures. Unexpectedly, both non-demineralized and demineralized chars showed similar reactivity, although former has higher mineral content. It was mentioned that some inorganic compounds showed catalytic effect on activation reaction [18], while some inorganic constituents in chars inhibit the activation reaction instead of catalyzing the activation.

In the case of the demineralized 450 °C chars, BET surface area increased over time up to 3 h, but no considerable influence was observed for surface area after 3 h. Micropore and mesopore volumes also showed the same trend over time. On the other hand, in the case of non-demineralized char, BET surface area of activated carbons increased continuously over time up to 4 h. From Table 2, it is clearly seen that demineralization enhanced the formation of micropores and mesopores. In the case of demineralized 600 °C chars, BET surface area increased over time up to 4 h, and then decreased. The activated carbon having highest surface area was obtained from 450 °C char, since this char contained less ash content than 600 °C char.

Martinez-Sanchez et al. studied the production of activated carbons from chromium tanned leather waste by CO_2 activation for different carbonization heating rates (1.5 and 5 °C/min), carbonization times (2 and 10 h) and activation times (8 and 28 h) [12]. They

observed that the micropore volume of the activated carbons did not change much with the carbonization and activation conditions. In addition, they produced the activated carbon from untanned leather to investigate the effect of tanning agent on pore structure of activated carbons. They stated that the presence of chromium to an extent led to development in pore structure of activated carbons. But, excess amount of tanning agent limited development in pore structure of activated carbons due to the blockage of Cr_2O_3 particles.

Oliveria et al. also prepared activated carbon from chromium-containing solid waste by CO_2 activation for an activation time of 0.5 h and 2 h at 850 °C [13]. They obtained the activated carbon with BET surface area of 889 m²/g and micropore volume of 0.39 cm³/g. The difference in micropore volume of activated carbons obtained in our study and in the study of Oliveria may be due to the particle size of the chromium oxide on activated carbon. Although we have not determined the size of chromium oxide on the activated carbon, Oliveria et al. reported that the chromium oxide was nanodispersed on the activated carbon.

3.1.2. Chemical activation

The advantage of chemical activation over physical activation is that it can be performed in only one step and at a relatively low temperature. In chemical activation, the yield and properties of activated carbon depend mainly on chemical agent, impregnation ratio and activation temperature. In this study, the CTS was impregnated with different concentrations of $ZnCl_2$ and H_3PO_4. The impregnated samples were pyrolyzed at 450 and 600 °C. The effect of carbonization temperature and reagent concentration on the yield, ash content, and BET surface area of activated carbon obtained from chemical activation by $ZnCl_2$ and H_3PO_4 are given in Tables 3 and 4, respectively.

As seen from Table 3, in the case of $ZnCl_2$ activation, surprisingly, almost no activation effect was observed at 450 °C. This may be due to the fact that $ZnCl_2$ cannot react with collagen at low temperature. $ZnCl_2$ showed an activation effect at high temperature. The surface area of activated carbons continuously decreased with impregnation ratio. In contrast to $ZnCl_2$, an activation effect was observed with H_3PO_4 at 450 °C. At this temperature, the surface area and porosity decreased with increase of H_3PO_4 amount (Table 4).

Impregnation with $ZnCl_2$ and H_3PO_4 led to a decrease in the yield of resulting carbon as a result of promoted gasification of the char, although impregnation agents retard escape of tar during carbonization [19]. This result is in agreement with the observations of other workers studied with lignocellulosic materials [20,21]. It was also noted that, for both zinc chloride and phosphoric acid, the impregnation ratio appears to have no considerable effect on the yield of activated carbon in this study.

The ash content of activated carbons obtained with zinc chloride impregnation was lower than the ash content of raw chars obtained without impregnation. This fact confirms that the inor-

Table 3
BET surface area, pore volumes and average pore size of activated carbons obtained from chemical activation of CTS with $ZnCl_2$.

Carbonization temperature, °C	Reagent concentration, wt%	Yield, wt%	Ash, wt%	BET surface area, m^2/g	Micropore volume, cm^3/g	Mesopore volume, cm^3/g	Total pore volume, cm^3/g	Average pore size, Å
450	–	35.1	11.6	N.D.	N.D.	N.D.	N.D.	N.D.
	50	33.3	7.4	N.D.	N.D.	N.D.	N.D.	N.D.
	100	28.7	8.6	20	–	0.112	0.087	17.3
	150	28.4	12.1	5	–	0.230	0.159	11.8
600	–	33.4	17.1	N.D.	N.D.	N.D.	N.D.	N.D.
	50	31.2	10.8	821	0.333	0.065	0.382	9.3
	100	31.8	11.9	730	0.368	0.074	0.406	11.1
	150	32.6	12.8	556	0.278	0.119	0.342	12.3

N.D.: not determined.

Table 4
BET surface area, pore volumes and average pore size of activated carbons obtained from chemical activation of CTS with H_3PO_4.

Carbonization temperature, °C	Reagent concentration, wt%	Yield, wt%	Ash, wt%	BET surface area, m^2/g	Micropore volume, cm^3/g	Mesopore volume, cm^3/g	Total pore volume, cm^3/g	Average pore size, Å
450	–	35.1	11.6	N.D.	N.D.	N.D.	N.D.	N.D.
	50	23.3	7.2	670	–	0.866	0.850	50.8
	100	21.7	9.8	364	0.073	0.311	0.333	36.7
	150	25.7	26.8	262	0.061	0.179	0.225	34.4
600	–	33.4	17.1	N.D.	N.D.	N.D.	N.D.	N.D.
	100	27.9	20.2	505	0.120	0.167	0.292	23.1

N.D.: not determined.

ganic constituent of the raw material combined with zinc chloride gives water- and HCl-soluble components.

3.2. Production of activated carbon from vegetable tanned leather shaving waste

3.2.1. Physical activation

For production of activated carbon from vegetable tanned leather shaving waste by physical activation, the demineralized chars obtained from carbonization at 600 °C were treated with CO_2 gas at 900 °C for 1–4 h.

The effect of activation time on the degree of burn-off, BET surface area and pore volumes of demineralized char is given in Table 5. Because of the high burn-off value, the activation times more than 4 h were not tested. As it can be discerned from Table 5, the BET surface area, micropore volume and mesopore volume of activated carbons increased continuously over time. It is clearly seen that after 2 h, activated carbon gained more mesopore character.

By comparison of results in Tables 2 and 5, it is seen that BET surface area (maximum) of activated carbon obtained from VTS is approximately two times higher than that from CTS. The reason may be the inhibiting effect of chromium on gasification and/or high ash content leading to pore blockage. By demineralization, the ash content of VTS-derived 600 °C char was decreased from 11.2% to 4.2% corresponding to a decrease ratio of approximately 62.5%. However, the ash content of CTS-derived 600 °C char could not be considerably reduced as mentioned in Section 3.1.1. Therefore,

Table 5
The effect of activation time on burn-off, BET surface area, pore volumes and average pore sizes of activated carbons from VTS-derived demineralized 600 °C chars.

Activation time, h	1	2	3	4
Burn-off, %	27.2	39.2	53.4	67.7
BET surface area, m^2/g	263	703	992	1205
Micropore volume, cm^3/g	N.D.	0.206	0.268	0.315
Mesopore volume, cm^3/g	N.D.	0.107	0.214	0.394
Total pore volume, cm^3/g	N.D.	0.332	0.498	0.705
Average pore size, Å	N.D.	18.9	20.1	23.4

N.D.: not determined.

demineralization was observed to be more effective for the VTS-derived 600 °C char and led to formation of activated carbons with high surface area and good porosity related highly to the absence of chromium in VTS.

3.2.2. Chemical activation

For the production of activated carbon from VTS by chemical activation method, $ZnCl_2$ and H_3PO_4 were used as impregnating agents, as in the case of CTS. The effect of carbonization temperature and reagent concentration on the yield, ash content, and BET surface area of activated carbon are given in Tables 6 and 7.

In the case of $ZnCl_2$, increase in activation temperature resulted in the increase of surface area of activated carbons. This result was attributed to possible increase in tar gasification [22]. As the amount of $ZnCl_2$ increased, mesopore volume increased, while micropore volume decreased. Similar trend was observed for the production of activated carbon from lignocellulosic material [23]. According to Caturla, at high $ZnCl_2$ concentrations, some $ZnCl_2$ remains in the external part of the carbon particles and widens the porosity by a localized decomposition of the organic matter [23], which results in the enhancement of the meso- and macro-pore formation. On the other hand, Ahmadpour et al. described pore evolution with respect to the activating agent concentration and showed that micropore formation was predominant when the $ZnCl_2$ to precursor mass ratio was less than 1:1 [24]. At impreg-nation ratios in the range of 1:1–2:1, they observed creation and widening of the micropores simultaneously. When the impreg-nation ratio was greater than 2:1, pore widening became the dominant mechanism and formation of mesopores became favor-able. It can be deduced that pore widening takes place at the expense of micropore formation for high $ZnCl_2$-to-waste ratios, thereby reducing the micropore content and increasing the meso-pore content. In our study, the effect of impregnation ratio on the surface areas of activated carbons was found to be dependent on the activation temperature. At both activation temperature, higher impregnation ratio (>150 wt%) led to a decrease in carbon yield as a result of promoted gasification.

In contrast to $ZnCl_2$ activation, activated carbons obtained at 450 °C had higher surface area than the activated carbons obtained

Table 6
BET surface area, pore volumes and average pore size of activated carbons obtained from chemical activation of VTS with $ZnCl_2$.

Carbonization temperature, °C	Reagent concentration, wt%	Yield, wt%	Ash, wt%	BET surface area, m²/g	Micropore volume, cm³/g	Mesapore volume, cm³/g	Total pore volume, cm³/g	Average pore size, Å
450	–	45.6	2.3	N.D.	N.D.	N.D.	N.D.	N.D.
	50	45.2	4.2	878	0.247	0.157	0.426	19.4
	100	44.6	3.6	1093	0.248	0.277	0.545	19.9
	150	42.0	4.0	1007	0.171	0.478	0.647	25.7
	200	37.7	3.9	674	0.160	0.518	0.683	40.5
600	–	41.6	4.2	N.D.	N.D.	N.D.	N.D.	N.D.
	100	39.2	1.5	1097	N.D.	N.D.	N.D.	N.D.
	150	40.9	1.9	1224	N.D.	N.D.	N.D.	N.D.
	200	33.8	2.3	1274	–	1.351	1.385	48.9

N.D.: not determined.

Table 7
BET surface area, pore volumes and average pore size of activated carbons obtained from chemical activation of VTS with H_3PO_4.

Carbonization temperature, °C	Reagent concentration, wt%	Yield, wt%	Ash, wt%	BET surface area, m²/g	Micropore volume, cm³/g	Mesapore volume, cm³/g	Total pore volume, cm³/g	Average pore size, Å
450	–	45.6	2.3	N.D.	N.D.	N.D.	N.D.	N.D.
	50	44.9	5.6	493	0.146	0.123	0.283	22.9
	100	42.5	2.9	774	0.232	0.274	0.503	26.0
	150	39.4	3.1	855	0.229	0.358	0.595	27.9
600	–	41.6	4.2	N.D.	N.D.	N.D.	N.D.	N.D.
	100	48.1	9.2	543	N.D.	N.D.	N.D.	N.D.

N.D.: not determined.

at 600 °C for the same activating agent concentration (100 wt%) in the case of H_3PO_4 activation. Phosphoric acid functions both as an acid catalyst to promote bond cleavage and the formation of cross-links via cyclization and condensation reactions, and to combine with organic species to form phosphate and polyphosphate bridges that connect and cross-link biopolymer fragments. The existence of phosphate groups causes a dilation in the structure and the removal of these groups by washing leaves the carbon matrix in an expanded state with an accessible pore structure. At temperatures above 450 °C, a secondary contraction of the structure occurs when the phosphate linkages become thermally unstable. The reduction in cross-link density allows the growth and alignment of polyaromatic clusters, producing a more densely packed carbon structure with some reduction in porosity [25]. So a possible reduction in porosity due to structural contraction seems to be the reasonable explanation for the reduced surface area of activated carbon produced by H_3PO_4 activation at 600 °C. It should be pointed out that the ash contents in activated carbons obtained with $ZnCl_2$ and even with H_3PO_4 were significantly low. Only activated carbon obtained with H_3PO_4 activation at 600 °C had high ash content possibly due to the incorporation of phosphate species to the carbon matrix. However, at low temperature activation, all the phosphorus in activated carbon could be removed with washing due to the absence of the bonding of the phosphorus to the carbon structure.

3.3. SEM analysis of activated carbons

Generally, with the SEM micrographs, it is possible to observe the macropore domain of activated carbons. The micropores are not visible at the magnification of the SEM, since they are characterized in the region of size equal to or less than 2 nm.

SEM images of activated carbons produced from non-demineralized and demineralized chars obtained by carbonization of CTS at 450 °C and 600 °C, are given in Figs. 1 and 2, respectively. It is clearly seen that there are white particles aggregated and dispersed on the carbon surfaces in all micrographs. In Fig. 3, EDX analysis of the two different regions of the activated carbon produced from 600 °C demineralized char is presented. It is clearly
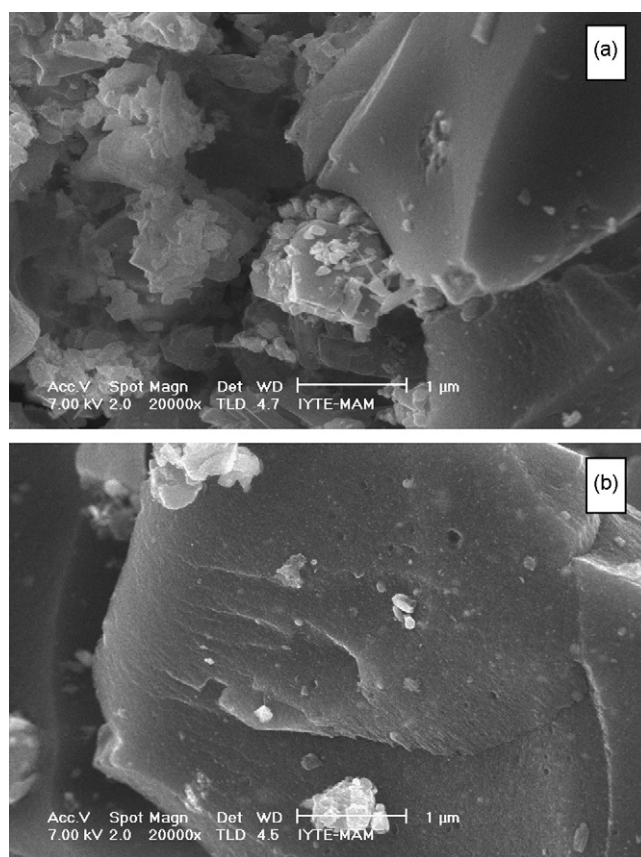

Fig. 1. SEM micrographs of activated carbons produced by physical activation of CTS-derived 450 °C char for 3 h (a) non-demineralized 450 °C char (at 20,000× magnification) and (b) demineralized 450 °C char (at 20,000× magnification).
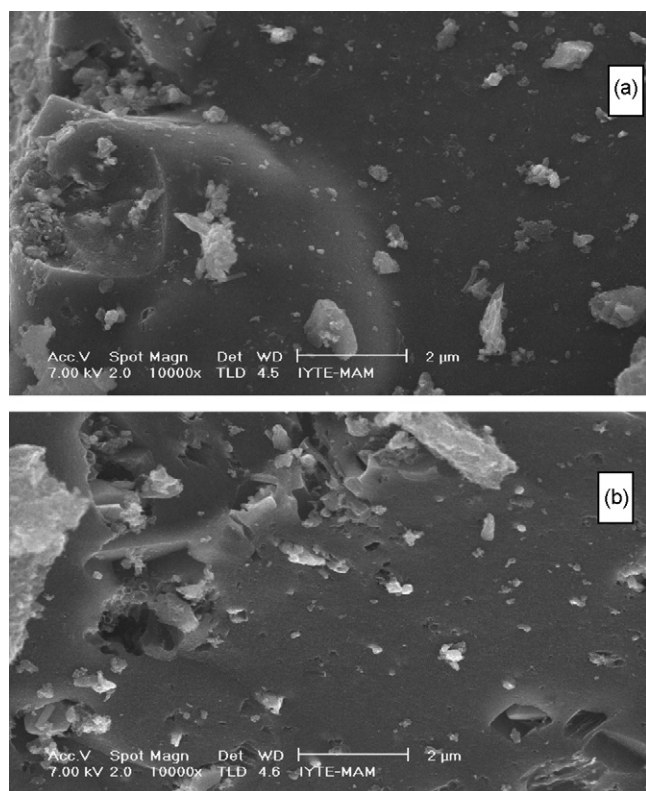
Fig. 2. SEM micrograph of activated carbon produced by physical activation of CTS-derived 600 °C char for 3 h (a) non-demineralized 600 °C char (at 20,000× magnification) and (b) demineralized 600 °C char (at 20,000× magnification).

seen that the inorganic constituents (white particles) on activated carbon contained considerable amount of chromium.

SEM images of activated carbons produced from CTS by chemical activation with $ZnCl_2$ (50 wt%) at 600 °C and with H_3PO_4 (50 wt%) at 450 °C are given in Fig. 4a and b, respectively. It is clearly seen that activated carbon obtained by H_3PO_4 activation has more developed porosity.

SEM images of activated carbons produced from VTS are given in Figs. 5–7. As seen from these figures, activated carbons produced by physical activation and chemical activation with H_3PO_4 appear to have some macroporosity. In contrast, activated carbon produced by chemical activation with $ZnCl_2$ appears to have no macroporosity.

3.4. Adsorption from aqueous solutions

Aqueous adsorption tests were conducted on selected activated carbons with the aim of assessing potential applications in the water-treatment industry. Three adsorbates, methylene blue, phenol, and Cr(VI), which are common toxic contaminants in waste waters, were used in this study. The activated carbons produced from vegetable tanned shaving were used as adsorbents. The activated carbon obtained from 600 °C demineralized char by physical activation for 4 h was donated as VPC, while the activated carbons obtained at 450 °C by chemical activation with $ZnCl_2$ (100 wt%) and H_3PO_4 (150 wt%) were donated as VZC and VHC, respectively.

3.4.1. Adsorption of methylene blue

In this group of experiments, optimum equilibrium time and pH was determined as 24 h and natural pH of the solution according to the preliminary studies, respectively. The isothermal equilibrium data obtained were processed by employing Langmuir and Freundlich isotherm equations. Table 8 shows the Langmuir and
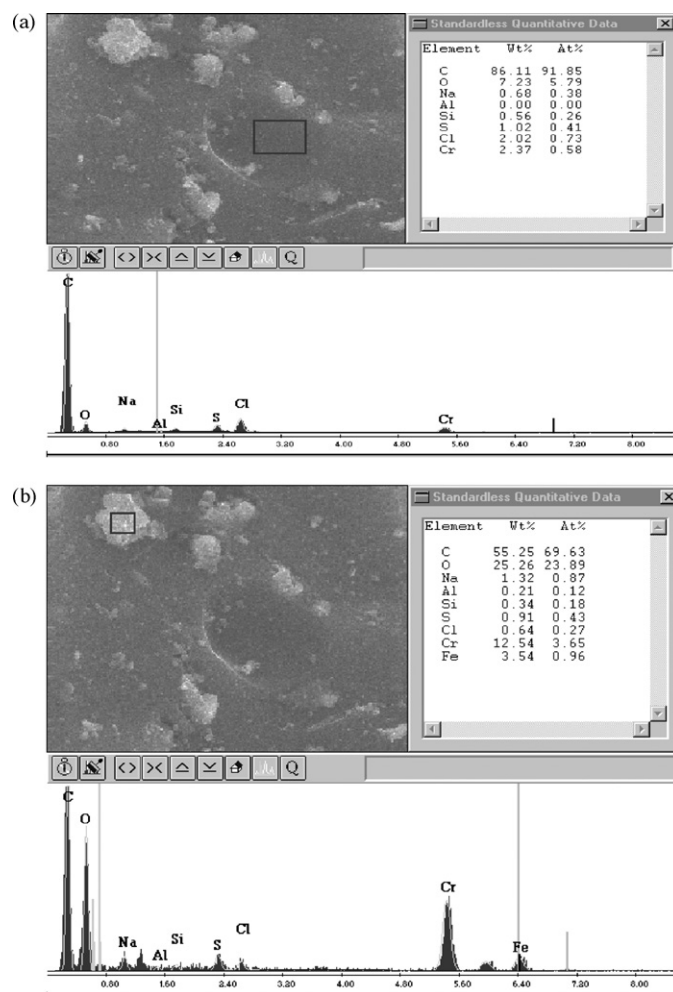

Fig. 3. EDX patterns – a and b – of two different parts of activated carbon produced from CTS-derived demineralized 600 °C char.

Freundlich parameters obtained by fitting data of the methylene blue adsorption on activated carbons. The Langmuir isotherms generated a satisfactory fit to the experimental data ($R^2 > 0.99$) for all tested activated carbons. This demonstrates monolayer coverage of methylene blue at the outer surface of the adsorbent. By examining Table 8 together with Tables 5–7, it is seen that there is a correlation between BET surface area and methylene blue adsorption. The methylene blue molecule has a minimum molecular cross-section

Table 8
Parameters of the Langmiur and Freundlich adsorption models of methylene blue, phenol, and Cr(VI).

| Activated carbon	Langmuir model			Freundlich model		
	S_M, mg/g	K_L, l/mg	R^2	$1/n$, mg/g	K_f, l/mg	R^2
Methylene blue						
VPC	416.7	1.142	0.99	0.075	308.3	0.98
VZC	400.0	0.892	0.99	0.080	288.6	0.99
VHC	357.2	0.757	0.99	0.173	178.4	0.91
Phenol						
VPC	147.1	0.106	0.99	0.336	32.6	0.99
VZC	99.0	0.013	0.73	0.502	5.3	0.90
VHC	105.2	0.025	0.91	0.395	11.9	0.96
Cr(VI)						
VPC	126.6	0.157	0.99	0.238	42.3	0.99
VZC	138.9	0.060	0.99	0.384	22.0	0.99
VHC	133.3	0.067	0.98	0.348	25.0	0.99
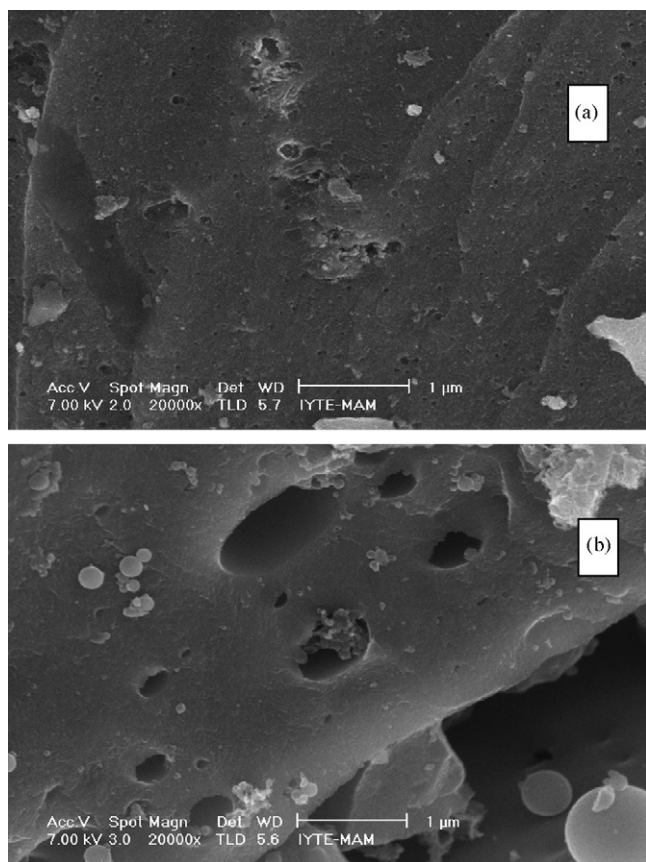
Fig. 4. SEM micrographs of activated carbon produced from CTS by chemical activation (a) with ZnCl$_2$ (100 wt%) at 600 °C and (b) with H$_3$PO$_4$ (50 wt%) at 450 °C.

Fig. 5. SEM micrographs of activated carbon produced by physical activation of demineralized 600 °C VTS char for 4 h (at 5000× and 10,000× magnification).

of about 0.8 nm and the minimum pore diameter of activated carbon accessible to methylene blue was estimated as 1.3 nm [26]. Therefore, it has access to the largest micropores and most of it is likely to be adsorbed in mesopores [27]. The activated carbons prepared in this study showed high methylene blue adsorption capacity due to their mesoporous characteristic.

Comparison of methylene blue adsorption capacities of activated carbons obtained in this study with the more traditionally used lignocellulosic materials may be made.

The methylene blue adsorption capacities of activated carbon prepared from olive seed waste residue [27], pine cone [28], date pits [29], oreganum stalks [30], and rice straw [31] were found to be 262 mg/g, 370.3 mg/g, 240 mg/g, 333.3 mg/g and 820 mg/g, respectively.

3.4.2. Adsorption of phenol

In this study, phenol adsorption equilibrium experiments were carried out at natural pH of the solution and for an equilibrium time of 4 h, which were determined as optimum according to the preliminary studies.

Table 8 shows the values of Langmuir and Freundlich isotherms parameters. As seen from Table 8, activated carbon obtained by phosphoric acid activation (VHC) fits only Freundlich equation indicating that significant adsorption takes place at low concentrations. The parameter n was found to be close to 2.5, which shows the favorability of phenol adsorption [32]. In the case of activated carbon obtained by physical activation (VPC), both equations were found to fit the data well ($R^2 = 0.99$).

Phenol (size of phenol ≈ 0.8 nm) is assumed to be adsorbed mainly within the micropores. However, the micropore volume alone is not sufficient to explain the differences in adsorption
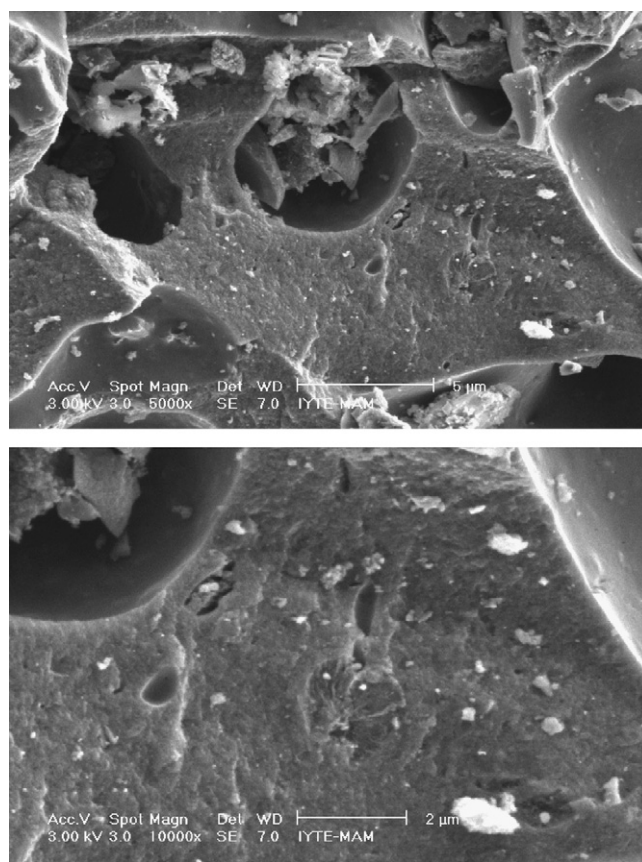
capacities of activated carbons. The relative affinity of the phenolic compound toward the carbon surface was related to the donor–acceptor complexes formed between the basic sites on the carbon surface and the organic ring of the phenol as well as the surface area and the porosity of the carbon [33]. The effect of basic surface oxygen groups on the adsorption of phenol was reported in the literature [34–36]. Since VPC has the highest micropore volume and highest number of surface basic groups (Table 9), it showed the highest phenol adsorption capacity. The phenol adsorption capacity of VPC was even higher than the adsorption capacity of activated carbon produced from oreganum stalk, vetiver roots and nutshell by chemical activation [30,37,38]. But, it was lower than the derived from coconut shell and lignin by chemical activation [39,34] and from pinewood by steam activation [40].

3.4.3. Adsorption of Cr(VI)

Metal adsorption is dependent on pH highly related to the type and ionic state of the functional group present in the adsorbent and also to the metal chemistry in the solution, besides the porosity and surface area of adsorbent. Cr(VI) adsorption equilibrium experiments were carried out at pH = 2 which was determined as optimum according to the preliminary studies. High adsorption of Cr(VI) at low pH can be explained by the species of the Cr and the

Table 9
Total amounts of surface acidic and basic sites of activated carbons.

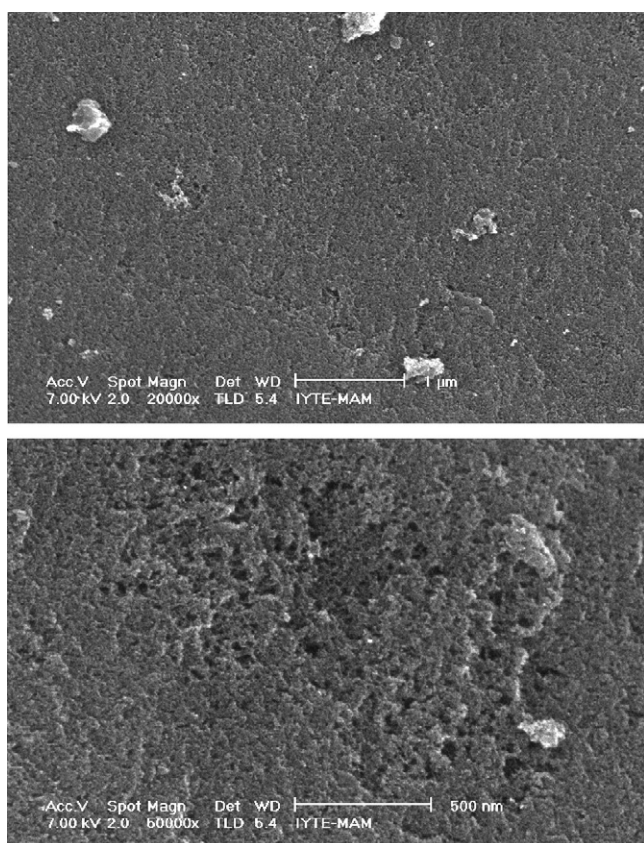| Activated carbon	Total acidic sites, mmol H$^+$/g AC	Total basic sites, mmol OH$^-$/g AC
VPC	1.30	1.51
VZC	2.00	0.55
VHC	0.05	0.33

Fig. 6. SEM micrographs of activated carbon produced from VTS by chemical activation with $ZnCl_2$ (200 wt%) at 600 °C (at 20,000× and 50,000× magnification).

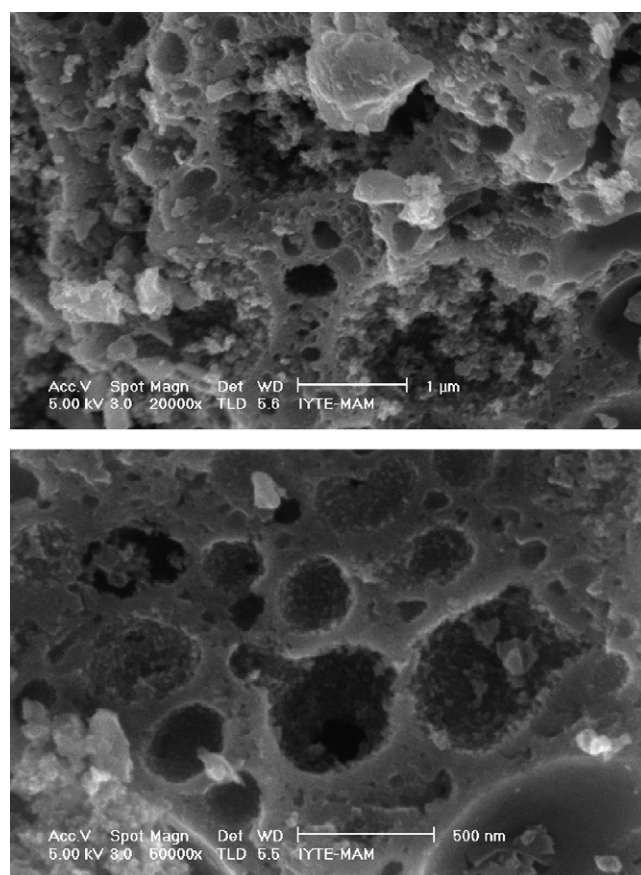**Fig. 7.** SEM micrographs of activated carbon produced from VTS by chemical activation with H_3PO_4 (150 wt%) at 450 °C (at 20,000× and 50,000× magnification).

adsorbent surface. It is reported that the predominant species of Cr in solution are $Cr_2O_7^{2-}$, $HCrO_4^-$, $Cr_3O_{10}^{2-}$ and $Cr_4O_{13}^{2-}$ at acidic pH [41]. Under acidic conditions, the surface of the activated carbons becomes highly protonated and favors the uptake of Cr(VI) in the anionic form.

The equilibrium datas fits both the Langmuir and Freundlich equations well for all three carbons (Table 8). Langmuir Cr(VI) adsorption capacities of activated carbons are almost similar, although they have different surface area and micropore volume. The reason may be attributed to the simultaneous effect of surface groups, pore structure, and surface area of activated carbons.

It must be noted that the activated carbons obtained in this study had higher Cr(VI) adsorption capacities than most of the commercial and lignocellulosic material-derived activated carbons found in literature [34,42–49].

4. Conclusion

In this study, the activated carbons were prepared from leather (chromium and vegetable tanned) shaving wastes by physical and chemical activation methods. In comparison with chromium tanned leather shaving waste, the vegetable tanned leather shaving waste produced activated carbon with a higher surface area and micropore volume by both physical and chemical activation processes. In physical activation process, the chromium in chromium tanned leather shaving led to high ash content and inhibition of gasification.

In the case of chromium tanned shaving, activated carbon with a surface area of 796 $m^2 g^{-1}$ was obtained by physical activation. The chemical activation by $ZnCl_2$ and H_3PO_4 resulted in the activated carbons having surface area of 821 and 670 $m^2 g^{-1}$, respectively.

In the case of vegetable tanned shaving, activated carbon with a surface area of 1205 $m^2 g^{-1}$ was obtained by physical activation, whereas activated carbons with the surface area of 1274 and 855 $m^2 g^{-1}$ were obtained by $ZnCl_2$ and H_3PO_4 activation, respectively.

The aqueous adsorption tests were also carried out with the activated carbons obtained from vegetable tanned shaving. Adsorption capacities of activated carbons for methylene blue and Cr(VI) were found to be higher than that of most of lignocellulosic material-derived activated carbons found in literature.

As conclusion, the present study showed that solid wastes from tannery industry can be effectively used as a raw material for the preparation of activated carbon by physical and chemical activation. And, it was proposed that produced activated carbons show promise for the removal of dye, Cr(VI) and phenol from aqueous streams.

References

[1] T.A. Albanis, D.G. Hela, T.M. Sakellarides, T.G. Danis, Removal of dyes from aqueous solutions by adsorption on mixtures of fly ash and soil in batch and column techniques, Int. J. Global Nest. 2 (2000) 237–244.
[2] D.J. Joo, W.S. Shin, J.H. Choi, S.J. Choi, M.C. Kim, M.H. Han, T.W. Ha, Y.H. Kim, Decolorization of reactive dyes using inorganic coagulants and synthetic polymer, Dyes Pigm. 73 (2007) 59–64.
[3] N. Daneshvar, A.R. Khataee, M.H. Rasoulifard, M. Pourhassan, Biodegradation of dye solution containing Malachite Green: optimization of effective parameters using Taguchi method, J. Hazard. Mater. 143 (2007) 214–219.

[4] M. Ahmaruzzaman, D.K. Sharma, Adsorption of phenols from wastewater, J. Colloid Interface Sci. 287 (2005) 14–24.
[5] Y. Bayrak, Y. Yesiloglu, U. Gecgel, Adsorption behavior of Cr(VI) on activated hazelnut shell ash and activated bentonite, Micropor. Mesopor. Mater. 91 (2006) 107–110.
[6] S. Booth, A.J. Long, V.L. Addy, Converting tannery waste to energy, in: Visual Display Presentation, V-21, IULTCS II: Eurocongress, İstanbul, 24–27 May, 2006, accessed at http://www.aaqtic.org.ar/congresos/istanbul2006.
[7] K.J. Sreeram, S. Saravanabhavan, J.R. Rao, B.U. Nair, Use of chromium-collagen wastes for the removal of tannins from wastewaters, Ind. Eng. Chem. Res. 43 (2004) 5310–5317.
[8] A. Cassano, E. Drioli, R. Molinari, C. Bertolutti, Quality improvement of recycled chromium in the tanning operation by membrane processes, Desalination 108 (1997) 193–203.
[9] D. Petruzzelli, R. Passino, G. Tiravanti, Ion exchange process for chromium removal and recovery from tannery wastes, Ind. Eng. Chem. 34 (1995) 2612–2617.
[10] L.F. Cabeza, M.M. Taylor, E.M. Brown, W.N. Marmer, Isolation of protein products from chromium-containing leather waste using two consecutive enzymes and purification of final chromium product: pilot plant studies, J. Soc. Leather Technol. Chem. 83 (1999) 14–19.
[11] L.F. Cabeza, M.M. Taylor, E.M. Brown, W.N. Marmer, Influence of pepsin and trypsin on chemical and physical properties of isolated gelatin from chrome shavings, J. Am. Leather Chem. Assoc. 92 (1997) 200–207.
[12] M.A. Martinez-Sanchez, C. Orgiles-Barcelo, J.M. Martin-Martinez, F. Rodriguez-Reinoso, Activated carbons from chromium-tanned leather waste, in: G.L. Ferrero, K. Maniatis, A. Buekens, A.V. Bridgewater (Eds.), Pyrolysis and Gasification, Elsevier, London, 1989, pp. 439–443.
[13] L.C.A. Oliveira, M.C. Guerreiro, M. Gonçalves, D.Q.L. Oliveira, L.C.M. Costa, Preparation of activated carbon from leather waste: a new material containing small particle of chromium oxide, Mater. Lett. 62 (2008) 3710–3712.
[14] O. Yilmaz, I.C. Kantarli, M. Yuksel, M. Saglam, J. Yanik, Conversion of leather wastes to useful products, Resour. Conserv. Recy. 49 (2007) 436–448.
[15] G.J. Halsey, The rate of adsorption on a non-uniform surface, J. Phys. Chem. 16 (1948) 931.
[16] E.P. Barret, L.G. Joyner, P.P. Halenda, The determination of pore volume and area distributions in porous substances. I. Computations from nitrogen isotherms, J. Am. Chem. Soc. 73 (1951) 373–380.
[17] H.P. Boehm, E. Diehl, W. Heck, R. Sappok, Surface oxides of carbon, Angew. Chem. Int. Ed. 3 (1964) 669.
[18] P. Samaras, E. Diamadopoulos, G.P. Sakellaropoulos, The effect of mineral matter and pyrolysis conditions on the gasification of Greek lignite by carbon dioxide, Fuel 75 (1996) 1108–1114.
[19] H. Teng, T.S. Yeh, Preparation of activated carbons from bituminous coals with zinc chloride activation, Ind. Eng. Chem. Res. 37 (1998) 58–65.
[20] W.T. Tsai, C.Y. Chang, S.L. Lee, A low cost adsorbent from agricultural waste corn cob by zinc chloride activation, Bioresour. Technol. 64 (1998) 211–217.
[21] B.S. Girgis, M.F. Ishak, Activated carbon from cotton stalks by impregnation with phosphoric acid, Mater. Lett. 39 (1999) 107–114.
[22] J.V. Ibarra, R. Moliner, J.M. Palacios, Catalytic effects of zinc chloride in the pyrolysis of Spanish high sulphur coals, Fuel 70 (1991) 727–732.
[23] F. Caturla, M. Molina-Sabio, F. Rodriguez-Reinoso, Preparation of activated carbon by chemical activation with ZnCl$_2$, Carbon 29 (1991) 999–1007.
[24] A. Ahmadpour, D.D. Do, The preparation of activated carbon from macadamia nutshell by chemical activation, Carbon 35 (1997) 1723–1732.
[25] H. Marsh, F. Rodriguez-Reinoso, Activated Carbon, Elsevier, Oxford, 2006.
[26] A. Baçaoui, A. Yaacoubi, A. Dahbi, C. Bennouna, R. Phan Tan Luu, F.J. Maldonado-Hodar, et al., Optimization of conditions for the preparation of activated carbons from olive-waste cakes, Carbon 39 (2001) 425–432.
[27] G.G. Stavropoulos, A.A. Zabaniotou, Production and characterization of activated carbons from olive-seed waste residue, Micropor. Mesopor. Mater. 82 (2005) 79–85.
[28] G. Duman, Y. Onal, C. Okutucu, S. Onenc, J. Yanik, Production of activated carbon from pine cone and evaluation of its physical, chemical, and adsorption properties, Energy Fuels 23 (2009) 2197–2204.
[29] B.S. Girgis, A.A. El-Hendawy, Porosity development in activated carbons obtained from date pits under chemical activation with phosphoric acid, Micropor. Mesopor. Mater. 52 (2002) 105–117.
[30] S. Timur, I.C. Kantarli, J. Yanik, Preparation of activated carbons from Oreganum stalks by chemical activation, Energy Fuels 20 (2006) 2636–2641.
[31] G.H. Oh, C.R. Park, Preparation and characteristics of rice-straw-based porous carbons with high adsorption capacity, Fuel 81 (2002) 327–336.
[32] V. Fierro, V. Torné-Fernández, D. Montané, A. Celzard, Adsorption of phenol onto activated carbons having different textural and surface properties, Micropor. Mesopor. Mater. 111 (2008) 276–284.
[33] R.C. Bansal, M. Goyal, Activated Carbon Adsorption, CRC Press Inc., Boca Raton, FL, 2005.
[34] E. Gonzalez-Serrano, T. Cordero, J. Rodriguez-Mirasol, L. Cotoruelo, J.J. Rodriguez, Removal of water pollutants with activated carbons prepared from H$_3$PO$_4$ activation of lignin from kraft black liquors, Water Res. 38 (2004) 3043–3050.
[35] J.S. Mattson, H.B. Mark Jr., M.D. Malbin, W.J. Weber, J.C. Crittenden, Surface chemistry of active carbon: specific adsorption of phenols, J. Colloid Interface Sci. 31 (1969) 116–130.
[36] C. Moreno-Castilla, J. Rivera-Utrilla, M.V. Lopez-Ramon, F. Carrasco-Marin, Electrochemical reduction of graphite in LiClO$_4$-propylene carbonate electrolyte: influence of the nature of the surface protective layer, Carbon 35 (1995) 845–851.
[37] S. Altenor, B. Carene, E. Emmanuel, J. Lambert, J.J. Ehrhardt, S. Gaspard, Adsorption studies of methylene blue and phenol onto vetiver roots activated carbon prepared by chemical activation, J. Hazard. Mater. 165 (2009) 1029–1039.
[38] K. Mohanty, D. Das, M.N. Biswas, Preparation and characterization of activated carbons from Sterculia alata nutshell by chemical activation with zinc chloride to remove phenol from wastewater, Adsorption 12 (2006) 119–132.
[39] Z. Hu, M.P. Srinivasan, Preparation of high-surface-area activated carbons from coconut shell, Micropor. Mesopor. Mater. 27 (1999) 11–18.
[40] R. Tseng, F. Wu, R. Juang, Liquid-phase adsorption of dyes and phenols using pinewood-based activated carbons, Carbon 41 (2003) 487–495.
[41] B.M. Weckhuysen, I.E. Wachs, R.A. Schoonheydt, Surface chemistry and spectroscopy of chromium in inorganic oxides, Chem. Rev. 96 (1996) 3327–3349.
[42] D. Aggarwal, M. Goyal, R.C. Bansal, Adsorption of chromium by activated carbon from aqueous solution, Carbon 37 (1999) 1989–1997.
[43] S. Mor, K. Ravindra, N.R. Bishnoi, Adsorption of chromium from aqueous solution by activated alumina and activated charcoal, Bioresour. Technol. 98 (2007) 954–957.
[44] P. Alvarez, C. Blanco, M. Granda, The adsorption of chromium (VI) from industrial wastewater by acid and base-activated lignocellulosic residues, J. Hazard. Mater. 144 (2007) 400–405.
[45] S.X. Liu, X. Chen, X.Y. Chen, Z.F. Liu, H.L. Wang, Activated carbon with excellent chromium (VI) adsorption performance prepared by acid–base surface modification, J. Hazard. Mater. 141 (2007) 315–319.
[46] K. Ranganathan, Chromium removal by activated carbons prepared from Casurina equisetifolia leaves, Bioresour. Technol. 73 (2000) 99–103.
[47] M. Kobya, E. Demirbas, E. Senturk, M. Ince, Adsorption of heavy metal ions from aqueous solutions by activated carbon prepared from apricot stone, Bioresour. Technol. 96 (2005) 1518–1521.
[48] K. Mohanty, M. Jha, B.C. Meikap, M.N. Biswas, Removal of chromium (VI) from dilute aqueous solutions by activated carbon developed from Terminalia arjuna nuts activated with zinc chloride, Chem. Eng. Sci. 60 (2005) 3049–3059.
[49] Y. Guo, J. Qi, S. Yang, K. Yu, Z. Wang, H. Xu, Adsorption of Cr(VI) on micro- and mesoporous rice husk-based active carbon, Mater. Chem. Phys. 78 (2002) 132–137.